Impact of Solar Radiation on Chemical Structure and Micromechanical Properties of Cellulose-Based Humidity-Sensing Material Cottonid

Ronja Scholz (ronja.scholz@tu-dortmund.de)
Technische Universitat Dortmund https://orcid.org/0000-0001-9872-977X
Matthias Langhansl
Technical University Munich: Technische Universitat Munchen
Moritz Hemmerich
Hochschule Hamm-Lippstadt
Jörg Meyer
Hochschule Hamm-Lippstadt
Cordt Zollfrank
Technische Universität München: Technische Universitat Munchen
Frank Walther
Technische Universität Dortmund: Technische Universitat Dortmund

Research

Keywords: solar radiation, chemical structure, Cottonid, humidity-sensing material

Posted Date: October 19th, 2020

DOI: https://doi.org/10.21203/rs.3.rs-93091/v1

Version of Record: A version of this preprint was published at Functional Composite Materials on April 6th, 2021. See the published version at https://doi.org/10.1186/s42252-021-00022-4.

Impact of solar radiation on chemical structure and micromechanical properties of cellulose-based humidity-sensing material Cottonid

R. Scholz[1,*], M. Langhansl[2], M. Hemmerich[3], J. Meyer[3], C. Zollfrank[2], F. Walther[1]

[1]Department of Materials Test Engineering (WPT), TU Dortmund University, Baroper Str. 303, D-44227 Dortmund, Germany (ronja.scholz@tu-dortmund.de, frank.walther@tu-dortmund.de)

[2]Biogenic Polymers, TUM Campus Straubing for Biotechnology and Sustainability, Schulgasse 16, D-94315 Straubing, Germany

[3]Photonics and Material Science, Hamm-Lippstadt University of Applied Science, Marker Allee 76-78, D-59063 Hamm, Germany

*corresponding author

Abstract

Renewable and environmentally responsive materials are an energy- and resource-efficient approach in terms of civil engineering applications, e.g. as so-called smart building skins. To evaluate the influence of different environmental stimuli, like humidity or solar radiation, on the long-term actuation behavior and mechanical robustness of these materials, it is necessary to precisely characterize the magnitude and range of stimuli that trigger reactions and the resulting kinetics of a material, respectively, with suitable testing equipment and techniques. The overall aim is to correlate actuation potential and mechanical properties with process- or application-oriented parameters in terms of demand-oriented stimuli-responsive element production. In this study, the impact of solar radiation as environmental trigger on the cellulose-based humidity-sensing material Cottonid, which is a promising candidate for adaptive and autonomously moving elements, was investigated. For simulating solar radiation in the lab, specimens were exposed to

short-wavelength blue light as well as a standardized artificial solar irradiation (CIE Solar ID65) in long-term aging experiments. Photodegradation behavior was analyzed by Fourier-transform infrared as well as electron paramagnetic resonance spectroscopy measurements to assess changes in Cottonid's chemical composition. Subsequently, changes in micromechanical properties on the respective specimens' surface were investigated with roughness measurements and ultra-micro-hardness tests to characterize variations in stiffness distribution in comparison to the initial condition. Also, thermal effects during long-term aging were considered and contrasted to pure radiative effects. In addition, to investigate the influence of process-related parameters on Cottonid's humidity-driven deformation behavior, actuation tests were performed in an alternating climate chamber using a customized specimen holder, instrumented with digital image correlation (DIC). DIC was used for precise actuation strain measurements to comparatively evaluate different influences on the material's sorption behavior. The infrared absorbance spectra of different aging states of irradiated Cottonid show decreased absorption at 2,900 cm^{-1}, i.e. the spectral region of C - H stretching vibrations, and increased absorption at 1,800-1,700 cm^{-1}, i.e. the spectral region of C = O stretching vibrations, with respect to unaged samples and therefore indicate oxidative stress on the surface. These findings differ under pure thermal loads. EPR spectra could corroborate these findings as radicals were detected, which were attributed to oxidation processes. Instrumented actuation experiments revealed the influence of processing-related parameters on the sorption behavior of the tested and structurally optimized Cottonid variant. Experimental data supports the definition of an optimal process window for stimuli-responsive element production. Based on these results, tailor-made functional materials shall be generated in the future where stimuli-responsiveness can be adjusted through the manufacturing process.

1. Introduction and state of the art

Stimuli-responsive materials inspired by the natural behavior of biological structures, like plants, are adaptive elements in various applications, viz. in biomedicine for drug delivery, in microfluidics and robotics as well as in bioarchitecture for development of e.g. climate-adaptive shading systems [1]. With regard to each application, different stimuli are relevant and, range e.g. from temperature and relative humidity to light and radiation. In bioarchitecture, the passive humidity-

driven shape change of cellulosic materials, like plants and wood, in reaction to changing environmental, i.e. weathering, conditions is used for an energy-efficient conversion of primary energy into a kinetic one. Consequently, it is in the nature of things, that these materials are additionally exposed to elevated temperatures and ultraviolet (UV) light during service, and it is of high relevance to characterize their thermal and radiation induced degradation behavior and its effect on their long-term material properties with regard to adaptive or constructive applications [2]. Since adaptivity to external stimuli, like temperature or relative humidity, is the condition for an efficient technical usage of weathering conditions within bioarchitecture, mostly polymer-based material systems, especially wood, are used for the development of so-called smart building skins [3].

In this context, Cottonid is a cellulose-based humidity-sensing material manufactured by the parchmentizing process, which exhibits great potential for the production of climate-adaptive elements with tailor-made material properties [4]. This study focusses the impact of solar radiation on chemical structure and micromechanical properties of the cellulose-based humidity-sensing material Cottonid. It is an extract of a comprehensive experimental study on the influence of individual manufacturing parameters on the functional and mechanical properties of the biopolymeric material by means of instrumented actuation and fatigue assessments. The results are used for application-oriented structural optimization of Cottonid for adaptive or constructive applications by adjustment of the manufacturing process.

The results presented were obtained by a combination of non-destructive analytical and micromechanical investigations to build up a more profound knowledge about Cottonid's interaction with its environment and the effect of long-term exposure to weathering conditions on its structure-property-relationships on the exposed surface. In the next step, the effect on the macromechanical properties will be investigated by the help of instrumented quasi-static and fatigue experiments.

1.1 Thermal and light-induced degradation mechanisms in polymeric materials

As stated above, the properties of polymer-based material systems are affected by environmental effects and therefore extensive studies have been carried out in recent years on different stabilization strategies to improve their long-term behavior in technical applications. To avoid degradation, which manifests in e.g discoloration, pronounced decrease of mechanical properties

and embrittlement, especially the addition of photostabilizers supports reasonable lifetimes in service, which in bioarchitecture means presence of elevated temperatures, changing degrees of relative humidity, influence of oxygen and solar radiation, while predictability of service lifetimes is the goal [5-7]. For cellulose, which is the most abundant biopolymer on earth and therefore intensively used as raw material for various stimuli-responsive material systems, the mechanism of photodegradation is induced by a superimposition of several radical reactions. An initial reaction is a decrease in degree of polymerization (DP) caused by scission of cellulose chains [8]. Yatagai and Zeronian investigated degradation mechanisms caused by ultraviolet (UV) irradiation, heat exposure and by a combination of both treatments. They revealed changes in color as well as formation of carbonyl, carboxyl and hydroperoxide groups, resulting in a decrease in α-cellulose content and degree of polymerization (DP). It was stated, that heat exposure alone caused reactions comparable to UV exposure [9]. Hon further observed a reaction of cellulosic carbon free radicals with oxygen molecules in electron paramagnetic resonance (EPR) studies, identifying oxygen as decisive reagent in photooxidative degradation of cellulose [10,11].

In case of cellulose-based material systems, wood is one of the most important engineering and structural materials. Infrared spectroscopy studies on wood exposed to UV irradiation observed an increased amount of carboxylic and carbonyl chromophoric functional groups and a decreased amount in aromatic functional groups, respectively. In these studies, mainly lignin-derived degraded products could be observed on specimens' surfaces. Nevertheless, as stated above, degradation by sunlight or UV radiation, resulting in pronounced structural modifications, is also expected for the other chemical components (cellulose, hemicelluloses). Though it could be verified, that these reactions were limited to the surface [12]. Efficient methods for characterizing these changes in chemical structure are Fourier transform infrared (FTIR) and electron paramagnetic resonance (EPR) spectroscopy, whereas EPR gives information about evolution of radicals related to radiation-induced degradation mechanisms and can be used to verify oxidation reactions that cause deviations from the initial IR spectra [13,14].

To characterize the impact of degradation mechanisms on the long-term behavior of cellulose-based material systems in bioarchitectural applications, a precise simulation of outdoor weathering conditions has to be performed in the lab. Solar radiation envelopes a range from 200 to 2500 nm, where irradiance levels are present in the visible part. For polymers, the UV part

of the spectrum, which reaches the earth's surface, is the most critical one [15]. Therefore, the influence of short-wavelength visible radiation as well as thermal loads on the long-term material properties in the already described application field is of high importance. Further, it is an advantage for research, if aging experiments could be accelerated while simultaneously not changing the temperature due to radiative energy input and hence keeping the causes for degradation viz. temperature and radiation separated. On this topic, Baltscheit et al. [16] and Hemmerich et al. [17,18] report on the simulation of the aging behavior of transparent materials under accelerated artificial conditions with prioritizing effects under blue light radiation with short-wavelength and high energy.

1.2 Bioinspired, stimuli-responsive materials for bioarchitectural applications

In response to external stimuli, like temperature, relative humidity or light etc., stimuli-responsive polymer-based material systems are able of autonomous reactions, e.g. adaptive shape changing, which is an energy-efficient way of producing kinetic energy or a mechanical force due to volume expansion. Therefore, nowadays in terms of energy-efficiency and eco-friendliness this bio-inspired mechanism is very interesting for implementation in technical and engineering issues. Applications fields are various and range from microfluidics over soft robotics to so-called bioarchitectural topics, where smart building skins respond to changing weathering conditions with adaptive reactions. E.g., with increasing temperature, single façade elements expand to provide shading and shrink, when temperatures are decreasing again, so that they are not permanently blocking the sight out of the building. In case of cellulose-based materials, like wood, the decisive stimulus, which activates the adaptive reactions, is humidity. Due to hygroscopic water uptake from the surrounding environment, cellulose micro fibrils swell perpendicular to their orientation within the material and cause a passive shape change, whose magnitude and direction is programmed in the microstructure [19]. This behavior can be observed for various plant systems, where the microstructure of the cell walls is used for directed swelling and shrinking processes [3,20]. These biological moving concepts have been an inspiration for the development of a variety of bio-inspired actuators for different applications in recent years to introduce the efficient relationship between structure and function by development of new functional materials [21-23]. The available actuation concepts, like one-dimensional bending, which is realized over bilayered systems, with one active and one passive layer with regard to the present stimulus, two-

dimensional stretching, buckling or three-dimensional volume expansion, can be adjusted by the microstructure of the polymer-based material systems and have their specific advantages and disadvantages with respect to the indented application. Also, a combination of these deformation modes in one actuator system is conceivable by microstructural tuning. Furthermore, the development of systems that respond to multiple external stimuli in a smart and foreseeable way is in the focus of current research [1,3,24]. Additionally, experiments with chemical degradation of matrix polymers to retain just the more porous cellulose scaffold for functionalization have been conducted. Besides usage of the dimensional instability when in contact with humidity in climate-adaptive building shells, the material behavior can also be used for production of curved timber elements by specific upstream humidity treatment and intelligent combination of layers with different micro fibril angles [19,25].

Therefore, smart building skins play an important role in the required global reduction of energy consumption, since autonomous, humidity-driven wood bilayers can serve as an energy-efficient alternative to motor-driven façade shading elements [26]. To assess the performance of the systems, especially the long-term stability as well as the repeatability of the humidity-driven movements, instrumented test setups, which simulate outdoor weathering conditions have been developed using environmental chambers and materials' reactions have been characterized, e.g. by optical monitoring of the swelling and shrinkage strains, measurements of changes in temperature, moisture content or other material specific parameters. Furthermore, the effect of different humidity cycles, slow and fast cycles in high and low humidity ranges, where investigated. During these experiments, a hysteresis was observed, when strains are plotted as function of relative humidity [27].

1.3 Cottonid material system

Cellulose as most abundant biopolymer on earth and therefore a very sustainable resource is an attractive material candidate for substitution of fossil products in specific, i.e. mostly functional, applications as stated above. Besides native cellulose, cellulose derivates, like e.g. regenerated or oxidized cellulose containing cellulose II crystals, are favored because of their simple and reproducible way of manufacturing. For this material class, the amount of inter- and intramolecular hydrogen bonds is very important for the physical properties of cellulosic commercial products [28]. For the above rendered adaptive applications, pure cellulosic materials often show a more

pronounced swelling and shrinking behavior in comparison to composite materials like wood. In this case, Cottonid is a modified natural material fully based on partly modified cellulose and appears to be a mix of cellulose I and II. Based on unsized raw paper, chemical modification is achieved by a treatment with a warm zincdichloride ($ZnCl_2$) or sulphuric acid (H_2SO_4) solution, called parchmentizing. The temperature of the catalyst bath T_{cat} and the reaction time t_{react} in it define the amount of inter- and intramolecular hydrogen bonds that are newly formed [4]. These are, as stated above, important for the final mechanical and physical properties. Since nowadays this well known material gains new relevance in technical and especially climate-adaptive applications, Scholz et al. performed an experimental assessment to qualify Cottonid in general for technical applications compared to established materials, like synthetic plastics and wood [29-31], as well as to assess the influence of individual manufacturing parameters on the amount of hydrogen bonds present and therefore on the functional and mechanical properties of Cottonid [32-34]. Furthermore, the impact of outdoor weathering conditions on the long-term actuation and fatigue behavior is characterized. The aim is to structurally optimize Cottonid [35] through adjustment of the manufacturing process for the production of Cottonid elements with tailor-made properties for either adaptive or constructive applications.

2. Materials and Methods

2.1 Sample preparation

For aging experiments, specimens were cut out of a plate of industrial Cottonid material (Ernst Krueger, Geldern, Germany) with a thickness of t_{mat} = 2.0 mm.

For actuation experiments, specimens were cut out of plates of the structurally optimized Cottonid variant M60Z50 with material thicknesses of $t_{mat,thin}$ = 0.4 mm and $t_{mat,thick}$ = 4.0 mm. Unsized raw paper (weight = 320 g/m^2, t_{mat} = 0.9 mm, Hahnemuehle, Dassel, Germany), which fully consists of cotton linters, subsequently marked as "M", was used for the production of M60Z50. For chemical treatment, a 70 wt-% zincdichloride ($ZnCl_2$) solution, subsequently marked as "Z", is used as catalyst. The sample name of the resulting Cottonid variants is a combination of the chosen manufacturing parameters (**Tab. 1**). The samples are then smoothed and dried in a calender (Sumet, Denklingen, Germany) under pressure and temperature. In order to prevent a dimensional change of the material due to water absorption from the environment, the samples

209 are stored under weight in a dry atmosphere until further analysis [33]. Caused by the
210 manufacturing process, the cellulose micro fibrils in the paper layers have a preferred orientation
211 in manufacturing direction [30]. So dependent on specimen location within the Cottonid sheet,
212 varying actuation and mechanical properties, respectively, are expected, **Fig. 1a**. Actuator type I
213 was chosen to characterize humidity-driven swelling and shrinking behavior perpendicular to
214 micro fibril axis, **Fig. 1b**.

215 For conditioning, specimens were stored under laboratory conditions (temperature T = 23 ± 2°C,
216 relative humidity φ = 35 ± 5%) for a time t_{cond} > 48 hrs before testing.

217 *2.2 Aging experiments*

218 The aging experiments were performed under certain combinations of temperature T and relative
219 humidity φ, which especially in case of φ were dependent on the used device but not controllable.
220 So, the changes in material properties discussed in this study are only relevant for these special
221 environmental parameters. Differences can be expected if higher humidities and/or higher
222 temperatures had been used in both the heat and UV exposures [8].

223 *2.2.1 Short-wavelength blue light and temperature*

224 Aging experiments under short-wavelength blue light were performed in a customized test setup
225 for accelerated optical aging of materials under predefined, constant conditions, developed by
226 [15-17]. The main component of the test setup is a double-wall specimen chamber out of high-
227 quality steel, which is thermostatted by a continuous circulation of water and equipped with
228 thermocouples for the measurement of temperature in the chamber and on the specimens'
229 surfaces. The cooling ensures, that specimens can be tempered between < 10°C and > 90°C
230 independent of the induced radiant power. For aging, a blue multi-chip-on-board high-
231 performance LED (CLU048-1818C4-B455-XX, Citizen Electronics, Kamikurechi, Japan) is
232 mounted above the specimen. The irradiance on the specimens' surfaces by the LED were
233 calculated using a raytracing simulation. By monitoring and saving of the operating parameters,
234 a controlled and traceable optical aging of specimens is realized [19].

235 Industrially manufactured Cottonid specimens for aging experiments have a unique red color
236 intended as marketing and recognition factor for the product. The temperature on surface due to
237 absorbtion (of the blue LED light) was T_{aging} ~75°C. Averaged irradiance was 12.8 kW/m^2 for an

aging time of t_{aging} = 3352 h. Relative humidity was measured directly after the LED was turned off and was φ_{LED} ~56%.

To separate degradation mechanism due to thermal and radiative loading, respectively, further specimens were thermally aged in an oven (UF 110 PLUS, Memmert, Schwabach, Germany) at T_{aging} = 75°C also for t_{aging} = 3352 h. Relative humidity was φ_{oven} ~0%.

2.2.2 Solar radiation

For simulation of solar radiation in the lab, in order to verify the comparability of LED irradiation in the blue spectral region, further specimens were exposed to standardized artificial solar radiation (CIE Solar ID65) in a commercial xenon weathering chamber (Suntest XLS+, Atlas, Altenhasslau) with averaged irradiance of 2 kW/m^2 for an aging time of t_{aging} = 3352 h. Temperature was T_{aging} = 75°C with a relative humidity of φ_{sun} ~11.2%

2.3 Structural investigations

2.3.1 Infrared and electron paramagnetic resonance spectroscopy

For analysis of changes in chemical structure due to thermal and light-induced degradation mechanisms, FTIR spectroscopy was utilized (Nicolet iS50, Thermo Fisher Scientific, Waltham, Massachusetts, USA). IR spectra after different durations of aging were obtained in the mid-IR range of 4000 to 400 cm^{-1} in attenuated total reflection mode (ATR). Since the reflection mode investigates the surface, a correlation with the ultra-micro-hardness measurements was possible. Twenty scans were averaged at a resolution of 4 cm^{-1}. A background scan was acquired for each sample and subtracted in the subsequent measurement. The software offers the possibility to correct the baseline drift and to automatically detect characteristic peaks.

For detection of organic radicals, which may form on the specimens' surfaces due to thermal and light-induced aging, electron paramagnetic resonance spectroscopy (EPR) (MiniScope MS 5000, Bruker, Billerica, Massachusetts, USA) was carried out on specimens aged with the standardized artificial solar irradiation (CIE Solar ID65). EPR spectra were obtained in a magnetic field range of 330 to 340 mT at a microwave frequency of f = 9.438 GHz and five measurements were averaged.

2.3.2 Surface roughness and ultra-micro-hardness testing

Surface roughness of the specimens was assessed with the profile method according to DIN EN ISO 4288 using a mobile surface roughness tester (MarSurf M 300 C, Mahr, Goettingen, Germany). For each aging state, roughness values were calculated and averaged based on three sampling lengths l_r = 2.5 mm.

Instrumented ultra-micro-hardness measurements were performed using a dynamic ultra-micro-hardness tester (DUH 211, Shimadzu, Kyoto, Japan) and load-indentation depth curves were obtained according to DIN EN ISO 14577. The process consists of a loading and unloading phases, where the load is applied with a constant load rate up to a predetermined indentation force of F_{max} = 98.09 mN. For each series of tests, five indentations per sample were made for each aging state. The change in Martens hardness ΔHM as well as indentation modulus E_{it} due to thermal and light-induced degradation processes was calculated and related to the values in initial condition.

2.4 Investigations on humidity-driven actuation behavior

For characterization of the humidity-driven swelling and shrinking behavior of the structurally optimized Cottonid variant M60Z50, static actuation test were performed in an alternating climate chamber (MKF 115, Binder, Tuttlingen, Germany) at a temperature $T_{climate}$ = 23°C and a relative humidity $\varphi_{climate}$ = 95% for a swelling time of t_s = 2.75 h, **Fig. 2a**. To allow for the hygroscopic expansion of the Cottonid specimen, a customized specimen holder was used, where one clamp is fixed and the other one is moveable, **Fig. 2b**. Actuation strains were measured using digital image correlation (DIC) (Limess, Krefeld, Germany), for this the specimens' surfaces were speckled with a traceable pattern, **Fig. 2c**. For optical monitoring of the movements, an encapsulated camera was used (Hero 5, GoPro, San Mateo, USA).

3. Results and Discussion

3.1 Infrared and electron paramagnetic resonance spectroscopy

Infrared spectra of the initial condition of Cottonid were depicted in relation to the aged states thermal (T_{aging} = 75°C for t_{aging} = 3352 h) in **Fig. 3**, optical (12.8 kW/m² at T_{aging} = 75°C for t_{aging} = 3352 h) in **Fig. 4** and sun (2 kW/m² at T_{aging} = 75°C for t_{aging} = 3352 h) in **Fig. 5**. The spectra were collected in a wavelength interval between 4,000 and 400 cm^{-1} and all of them show the

characteristic peaks for cellulose, which are defined in the initial condition spectra. In the interval between 3,600 and 3,100 cm^{-1} the stretching vibrations of the hydroxyl groups (v(-OH)) of the cellulose chains can be seen. The height and area of the peak provides information about inter- and intramolecular hydrogen bonds present in the material. The much lower peak at 2,900 cm^{-1} is attributed to the stretching vibrations of the alkyle groups (v(-CH)). Absorbed water is the reason for the peak at 1,640 cm^{-1}. In the interval between 1,300 and 900 cm^{-1} peaks of the alcohols located on the cellulose chains can be observed. The peak of the glycosidic linkage, which is also known as amorphous peak, can be found at 898 cm^{-1} [36].

When comparing the spectrum in initial condition with the spectra of the different aging states it becomes clear, that a considerable change in absorption can be detected at 2,900 cm^{-1} and between 1,750 and 1,740 cm^{-1}, respectively, which indicates the presence of oxidative stress on the surface for all aging states. The close-ups of the interesting regions make the changes more visible. The increase of peaks in the range of 1,750 and 1,740 cm^{-1} results from the formation of carbonyl and carboxyl groups due to reactions with the surrounding oxygen. These reactions imply the splitting of cellulose chains on the surface and a decrease of degree of polymerization (DP) [8-10,37]. Therefore, the peak at 2,900 cm^{-1} simultaneously decreases because of these oxidative reactions, indicating a degradation of C – H combinations. These findings could also be verified by EPR spectroscopy, since formation of organic radicals could be detected with increasing aging time, see **Fig. 6** [13]. The described reactions are most pronounced for specimens aged with the standardized artificial solar irradiation [8].

Another reaction worth mentioning is the increase of the peak at 1,644 cm^{-1}, which stands for adsorbed water. At first, it is not reasonable, that a specimen aged with temperature and light contains more water, since rather drying effects would be expected. Since the Cottonid specimens were taken out of the experimental setups for aging to collect IR and EPR spectra, the authors assume, that the material directly reacted with its surrounding again in taking up humidity from the ambient air.

3.2 Roughness and ultra-micro-hardness testing

Fig. 7 shows the results of roughness measurements for the initial condition in comparison to the different aging states.

For evaluation of the change of surface roughness due to thermal and light-induced aging, averaged roughness depth R_z and roughness value R_a were obtained. In general, the aged specimens seem to have a lower roughness and especially when looking at R_z, a pronounced difference is visible between initial and sun. This finding correlates with studies of Hauptmann et al., where a decrease of nanoroughness of wood due to UV-irradiation accompanied by a change in color was observed [38,39].

Results of ultra-micro-hardness tests are depicted in **Fig. 8**. Here, just three aging stages are shown since no results were available for the specimens aged with standardized artificial solar irradiation (sun). A maximum test force of F_{max} = 98.07 mN was chosen in order to evaluate an influence of thermal and light-induced aging on the micromechanical properties in the outer layers of the specimen. **Fig. 8a** displays load-displacement curves. Qualitatively, the aged specimens exhibit lower values in indentation depths. Furthermore, differences in the slope of the loading and unloading phase of each curve can be observed, which indicate a change in the elastic-plastic deformation behavior of the aged Cottonid specimens. For the purpose of comparability of the characteristic values Martens hardness HM and indentation modulus E_{it}, **Fig. 8b** shows the arithmetic mean and standard deviation of five measuring points for the initial condition, the thermal and the optical aged state. By comparison, the different aging states show pronounced differences within the characteristic values. Compared to the initial condition, thermally aged specimens show a distinct increase of HM and E_{it}, which is also visible for the optically aged specimens, but less pronounced. So, as expected, thermal and light-induced aging seems to lead to an embrittlement of the outer, irradiated layers of the specimens, which can be verified by several other studies on polymeric materials, especially wood [39].

3.3 Humidity-driven actuation

Fig. 9 shows the results of static actuation tests (T_{amb} = 23°C, φ_{amb} = 95% r.H., t_s = 2.75 h) on the structurally optimized Cottonid variant M60Z50. True tangential strain ε'_{Tan}, detected via DIC on the specimens' surfaces, is plotted over the swelling time t_s and the influence of material thickness t_{mat} as well as cellulose micro fibril orientation on the humidity-driven swelling and shrinking behavior is characterized. Strains parallel to cellulose micro fibril orientation (0°/X) are indexed with x, whereas strains perpendicular to cellulose micro fibril orientation (90°/Y) are indexed with y.

In **Fig. 9a**, results are shown for M60Z50 specimens with $t_{mat,\mathbf{thick}}$ = 4.0 mm and $t_{mat,\mathbf{thin}}$ = 0.4 mm. After a swelling time of t_s = 0.25 h, $\varepsilon'_{Tan,y,\mathbf{thin}}$ reaches its maximum with ~2.5% compared to $\varepsilon'_{T,y,\mathbf{thick}}$ with ~0.15%. So, while the thin specimen shows a very adaptive behavior, the thick one is more or less dimensionally stable. At the end of the test at t_s = 2.75 h $\varepsilon'_{Tan,y,\mathbf{thick}}$ increases up to ~0.4% compared to the initial condition. With regard to the thin specimen with ~2% at the end of the test, this humidity-driven expansion is much lower. So it can be concluded, that humidity-driven actuation behavior of Cottonid is a function of the material thickness t_{mat} and therefore by varying the amount of paper layers fed into the parchmentizing process either climate-adaptive elements for bioarchitectural issues or dimensionally stable components for conventional constructive issues can be produced. A transitional material thickness $t_{mat,trans}$, where humidity-driven expansions of Cottonid are not justifiable anymore with regard to standards for conventional construction, will be defined in further investigations.

In **Fig. 9b**, showing results for the M60Z50 specimen with $t_{mat,\mathbf{thin}}$ = 0.4 mm, it becomes clear, that swelling due to water absorption is more pronounced perpendicular to cellulose micro fibril orientation, since $\varepsilon'_{Tan,y,\mathbf{thin}}$ reaches a higher value of ~2.5% compared to $\varepsilon'_{Tan,x,\mathbf{thin}}$ = 1.5% after a swelling time of t_s = 0.25 h. After reaching its maximum value, $\varepsilon'_{Tan,y,\mathbf{thin}}$ decreases again and saturates after t_s = 0.75 h at ~2%. At t_s = 0.50 h, $\varepsilon'_{Tan,x,\mathbf{thin}}$ reaches its maximum, saturates at ~2.25% and stays above $\varepsilon'_{Tan,y,\mathbf{thin}}$ until the end of the test. It can be concluded, that for short swelling times, the Y-orientation is favorable, while there seems to be no distinct difference in the materials' reaction when it comes to long-term humidity loading.

4. Conclusions and Outlook

This study, focusing on the impact of solar radiation on chemical structure and micromechanical properties of the cellulose-based humidity-sensing material Cottonid, is an extract of a comprehensive experimental study on the influence of individual manufacturing parameters on the functional and mechanical properties of the biopolymeric material by means of instrumented actuation and fatigue assessments. It could be shown, that the impact of thermal loads in combination with solar radiation leads to chemical modifications of the cellulose on the surface of the aged Cottonid specimens. Infrared spectra revealed changes in adsorption at 2,900 cm^{-1}, i.e. the spectral region of C - H stretching vibrations, and between 1,800 and 1,700 cm^{-1}, i.e. the spectral region of C = O stretching vibrations, and therefore indicate oxidative stress on the

surface of the aged specimens [4,8,9]. These findings are underlined with results of EPR spectroscopy, which indicate the presence of oxidation-related radicals. The oxidative stress obviously provokes a decreased surface roughness leading to embrittlement, which could be verified by increased Martens hardness HM and indentation modulus E_{it} assessed by ultra-micro-hardness tests. Therefore, a change in micromechanical surface properties of the aged Cottonid specimens due to chemical modifications induced by a combination of thermal loads and solar irradiation could be observed [40-42]. Experiments with pure thermal loads induced comparable degradation effects to combined loads, whereas aging with a standardized artificial solar irradiation caused a more distinct material reaction compared to aging with short-wavelength blue light radiation [14]. These more or less material-specific reactions onto the induced loads could origin from the chemical modification of cellulose I in a not yet defined mix of cellulose I and II during the manufacturing process of Cottonid and have to be thoroughly investigated in further studies. Since for manufacturing of Cottonid the cellulose contained in the raw paper layers gets partly hydrolyzed by the help of an chemical catalyst, which was observed to be a stabilizing process in terms of light-induced radical reactions [8], these investigations will be of high interest to qualify Cottonid for outdoor applications. Further, since the presented results were obtained on industrial manufactured Cottonid material, which has a unique red color, it is essential to investigate and comparatively evaluate photodegradation mechanisms on colorless, i.e. white, Cottonid [8].

Actuation tests on the structurally optimized Cottonid variant M60Z50 revealed an influence of the material thickness t_{mat} as well as of the predefined orientation of the cellulose micro fibrils. It can be stated, that Cottonid's actuation behavior is a function of its material thickness, i.e. a ten times thinner specimen achieves a ten times increased humidity-driven expansion. Furthermore, humidity-driven actuation is more pronounced perpendicular to micro fibril orientation, which is already described in various studies concerning cellulose based materials [2,17,42]. These findings can be used for the development of climate-adaptive Cottonid elements capable of complex passive shape changes due to efficient and smart combination of microstructure and material thickness. Since Cottonid is manufactured by chemical modification of single paper layers, which are stacked to get thicker material, the adjustment and smart usage of these manufacturing parameters for tailor-made climate-adaptive element production can be easily implemented.

In summary, the conditions of the manufacturing process of Cottonid and its hygroscopic material behavior make the material ideal for the development of application-oriented adaptive elements capable of complex passive, humidity-driven shape changes with adjustable magnitude e.g. for bioarchitectural issues. The aging experiments revealed an interaction of Cottonid with thermal and light-induced loads, which are expected in natural weathering conditions, i.e. environmental triggers, in this application field. The change in micromechanical properties and degradation processes, respectively, on the surface have to be considered for the prediction of the long-term behavior of climate-adaptive Cottonid elements. Up to now the results show, that degradation takes place and that the modifications of the chemical structure also affect the micromechanical properties.

In further studies, it will be investigated how these mechanisms affect the macroscopic deformation behavior of Cottonid and its specific mechanical values, like Young's modulus and ultimate tensile strength, as well as the actuation behavior. For this, in a first step aging experiments will be conducted at different temperatures and relative humidity levels to assess the influence of weathering conditions on the degradation behavior. Furthermore, the customized specimen holder for actuation experiments can be equipped with LEDs, so that in the near future swelling and shrinking behavior can be characterized with superimposed thermal and light-induced loading.

Availability of data and materials

The datasets used and/or analyzed during the current study are available from the corresponding author on reasonable request.

Competing interests

The authors declare that they have no competing interests.

Funding

The authors thank the German Research Foundation (Deutsche Forschungsgemeinschaft, DFG) for funding the research project "Biomechanical qualification of the structure-optimized functional material Cottonid as an adaptive element" (WA 1672/23-1, ZO 113/22-1).

Author contributions

R.S., M.L. and M.H. performed experiments, prepared figures and wrote the manuscript. F.W., C.Z. and J.M. supervised the project.

Acknowledgements

The authors thank the Hahnmuehle FineArt GmbH (Dassel, Germany) and the Ernst Krueger GmbH & Co. KG (Geldern, Germany) for providing raw material for Cottonid manufacturing and industrial reference material. The assistance during lab work of Mr. T. Graszynski is greatfully acknowledged.

References

[1] M Wei, Y Gao, X Li, M J Serpe: Stimuli-responsive polymers and their applications. In: Polym. Chem. 8 (1), S. 127–143.

[2] M Rueggeberg, I. Burgert: Bio-inspired wooden actuators for large scale applications. PloS one 10(3), e0120718. doi: 10.1371/journal.pone.0120718.

[3] S Poppinga, C Zollfrank, O Prucker, J Ruehe, A Menges, T Cheng, T Speck, Toward a new generation of smart biomimetic actuators for architecture. Adv. Mater. 30(19), e1703653 (2018). doi: 10.1002/adma.201703653.

[4] T Taylor, U.S. patent 114,880, 16 March 1871.

[5] H Fan, G Li, F Yang, L Yang, S Zhang, Photodegradation of cellulose under UV light catalysed by TiO2. J. Chem. Technol. Biotechnol. 86(8), 1107-1112 (2011). doi: 10.1002/jctb.2632.

469 [6] E Yousif, R. Haddad, Photodegradation and photostabilization of polymers, especially
470 polystyrene: review. SpringerPlus 2(398), 1-32 (2013). doi: 10.1186/2193-1801-2-398.

471 [7] S Al-Malaika (ed.), Reactive modifiers for polymers – An A-Z reference. (Springer
472 Netherlands, 1997).

473 [8] T N Kleinert, Damage in cellulosic textiles caused by aging and light (in German). Lenz.
474 Rep. 25, 33-40 (1968).

475 [9] M Yatagai, S H Zeronian, Effect of ultraviolet light and heat on the properties of cotton
476 cellulose. Cellulose 1, 205-214 (1994).

477 [10] D N-S Hon, Photooxidative degradation of cellulose: Reactions of the cellulosic free
478 radicals with oxygen. J. Polym. Sci.: Polym. Chem. Ed. 17, 441-454 (1979).

479 [11] C Lin, T Zeng, Q Whang, l Huang, Y Ni, F Huang, X Ma, S Cao, Effects of the conditions
480 of the TEMPO/NaBR/NAClO system on the carboxyl groups, degree of polymerization,
481 and yield of the oxidized cellulose. BioRes 13(3), 5965-5975 (2018).

482 [12] D N-S Hon, S-T Chang, Surface degradation of wood by ultraviolet light. J. Polym. Sci.:
483 Polym. Chem. Ed. 22, 2227-2241 (1984).

484 [13] S Y Oh, D I Yoo, Y Shin, G Seo, FTIR analysis of cellulose treated with sodium hydroxide
485 and carbon dioxide. Carbohydr. Res. 340(3), 417-428 (2005). doi:
486 10.1016/j.carres.2004.11.027.

487 [14] F Schneider, K. Moebius, Analysis of electron resonance spectra of organic radicals (in
488 German). J. Nat. Res. (in German) 18b, 1111-1119 (1963).

489 [15] G Geuskens, in Degradation of polymers, ed. by C H Bamford, C F H Tipper (Elsevier
490 Scientific Pub. Co, New York, 1975), 420-424.

491 [16] J Baltscheit, N Schmidt, F Schroeder, J Meyer, Investigations on the aging behavior of
492 transparent bioplastics for optical applications. InfoMat 2(2), 424-433 (2020). doi:
493 10.1002/inf2.12065.

494 [17] M Hemmerich, R Scholz, S Saha, F Walther, J Meyer, Polylactid – a suitable bio-based
495 plastic for optical applications? - Test setup for accelerated optical and thermal aging.
496 special issue Chrom + Food Forum (03), 43-45 (2019).

[18] M Hemmerich, J Meyer, F Walther, Advanced test setup for accelerated aging of plastics by visible LED radiation, Mater. 13(1), 4261 (2020). doi: 10.3390/ma13194261.

[19] T Toratti, S. Svensson, Mechani-sorptive experiments perpendicular to grain under tensile and compressive loads. Wood Sci. Technol. 34, 317-326 (2000).

[20] I Burgert, T Keplinger, E Cabane, V Merk, R Rueggeberg, Biomaterial Wood: Wood-based and bioinspired materials. Sec. Xyl. Bio.: Origin, Functions, and Applications, 259-281 (2016). doi: 10.1016/B978-0-12-802185-9.00013-9.

[21] L Guiducci, J C Weaver, Y J M Bréchet, P Fratzl, J W C Dunlop, The geometric design and fabrication of actuating cellular structures. Adv. Mater. Inter. 2(11), 1500011 (2015). doi: 10.1002/admi.201500011.

[22] Q Zhu, Y Jin, W Wang, G Sun, D Wang, Bioinspired smart moisture actuators based on nanoscale cellulose materials and porous, hydrophilic EVOH nanofibrous membranes. ACS Appl. Mater. Inter. 11(1), 1440-1448 (2019). doi: 10.1021/acsami.8b17538.

[23] M Dai, O T Picot, J M N Verjans, L T de Haan, A P H J Schenning, T Peijs, C W M Bastiaansen, Humidity-responsive bilayer actuators based on a liquid-crystalline polymer network. ACS Appl. Mater. Inter. 5(11), 4945-4950 (2013). doi: 10.1021/am400681z.

[24] W Hilber, Stimulus-active polymer actuators for next-generation microfluidic devices. Appl. Phys. A 122(751), 1-40 (2016). doi: 10.1007/s00339-016-0258-6.

[25] P Groenquist, F K Wittel, M Rueggeberg, Modeling and design of thin bending wooden bilayers. PloS one 13(10), e0205607 (2018). doi: 10.1371/journal.pone.0205607.

[26] C Vailati, E Bachtiar, P Hass, I Burgert, M Rueggeberg, An autonomous shading system based on coupled wood bilayer elements. Energy Build. 158, 1013-1022 (2018). doi: 10.1016/j.enbuild.2017.10.042.

[27] A Patera, D Derome, M Griffa, J Carmeliet, Hysteresis in swelling and in sorption of wood tissue. J. Struct. Biol. 182(3), 226-234 (2013). doi: 10.1016/j.jsb.2013.03.003.

[28] Y Hishikawa, E Togawa, T Kondo, Characterization of individual hydrogen bonds in crystalline regenerated cellulose using resolved polarized FTIR Spectra. ACS Omega 2(4), 1469-1476 (2017). doi. 10.1021/acsomega.6b00364.

525 [29] C Fiedler Bremer, R Scholz, S Myslicki, P Starke, C Boller, F Walther, NDT-based
526 characterization of timber and vulcanized fiber for civil infrastructure. NDT-CE, 1-12
527 (2015).

528 [30] R Scholz, A Delp, A Kaplan, F Walther, Comparative evaluation of the temperature-
529 dependent mechanical properties of vulcanized fiber and technical plastics (in German),
530 Progression in Materials Testing for Research and Practice (in German). ed. by H-J
531 Christ. Conference Materials Testing, Neu-Ulm, December 2016. (Stahleisen,
532 Düsseldorf, 2016) 245-250.

533 [31] R Scholz, R-M Mittendorf, JK Engels, A Hartmaier, B Kuenne, F Walther, Direction-
534 dependent mechanical characterization of cellulose-based composite vulcanized fiber.
535 Mater. Test. 58(10), 813-817 (2016). doi: 10.3139/120.110929

536 [32] R Scholz, M Langhansl, C Zollfrank, F Walther, Cottonid – An efficient functional material
537 for humidity-driven actuators (in German). Smart Structures and Systems (in German),
538 ed. by T Melz, M Wiedemann. 4SMARTS-Symposiums, Darmstadt, May 2019 (Shaker,
539 Herzogenrath, 2019), 63-75.

540 [33] R Scholz, M Langhansl, C Zollfrank, F Walther, Experimental study on the actuation and
541 fatigue behavior of the biopolymeric material Cottonid. Mater. Tod.: Proc. 7, 476-483. doi:
542 10.1016/j.matpr.2018.11.112.

543 [34] R Scholz, M Langhansl, C Zollfrank, F Walther, Humidity-sensing material Cottonid –
544 Microstructural tuning for improved actuation and fatigue performance. Front. Mater. 7, 1-
545 10 (2020). doi: 10.3389/fmats.2020.00156.

546 [35] R Scholz, A Delp, F Walther, In situ characterization of damage development in Cottonid
547 due to quasi-static tensile loading. Mater. 13(9), 1-12 (2020). doi: 10.3390/ma13092180.

548 [36] V Hospodarova, E Singovszka, N Stevulova, Characterization of cellulosic fibers by FTIR
549 spectroscopy for their further implementation to building materials. AJAC 09(06), 303-310
550 (2018). doi: 10.4236/ajac.2018.96023.

551 [37] M Poletto, H L Ornaghi, A J Zattera: Native cellulose: structure, characterization and
552 thermal properties. Mater. 7(9), 6105-6119 (2014). doi: 10.3390/ma7096105.

553 [38] M Hauptmann, U Mueller, M Obersriebnig, W Gindl-Altmutter, A Beck, C Hansmann, The
554 optical appearance of wood related to nanoscale surfce roughness. Wood look &
555 roughness, BioRes 8(3), 4038-4045 (2013).

556 [39] L Gurau, H Mansfield-Williams, M Irle, Filtering the roughness of a sanded wood surface.
557 Int. Wood Prod. J. 64(5), 363-371 (2006). doi: 10.1007/s00107-005-0089-1.

558 [40] A O Rapp, C Brischke, C R Welzbacher, Interrelationship between the severity of heat
559 treatments and sieve fractions after impact ball milling: a mechanical test for quality
560 control of thermally modified wood. Wood res. (in German) 60(1), 64-70 (2006). doi:
561 10.1515/HF.2006.012.

562 [41] A Flores, N D Jordan, F J Baltà-Calleja, D C Bassett, R H Olley, N G Smith: Mechanical
563 changes linked to embrittlement at the wear surface of polyethylene implants in hip joints.
564 Polym. 41(21), 7635-7639 (2000). doi: 10.1016/S0032-3861(00)00132-4.

565 [42] M P Arrieta, J López (2013): Mechanical characterization of microlaminar structures
566 extracted from cellulosic materials using nanoindentation technique. Cellulose Chem.
567 Technol. 47(5-6), 345-351 (2013).

568 [43] M Frey, D Widner, J S Segmehl, K Casdorff, T Keplinger, I Burgert, Delignified and
569 densified cellulose bulk materials with excellent tensile properties for sustainable
570 engineering. ACS Appl. Mater. Inter. 10(5), 5030-5037. doi: 10.1021/acsami.7b18646.

571 **Figures**

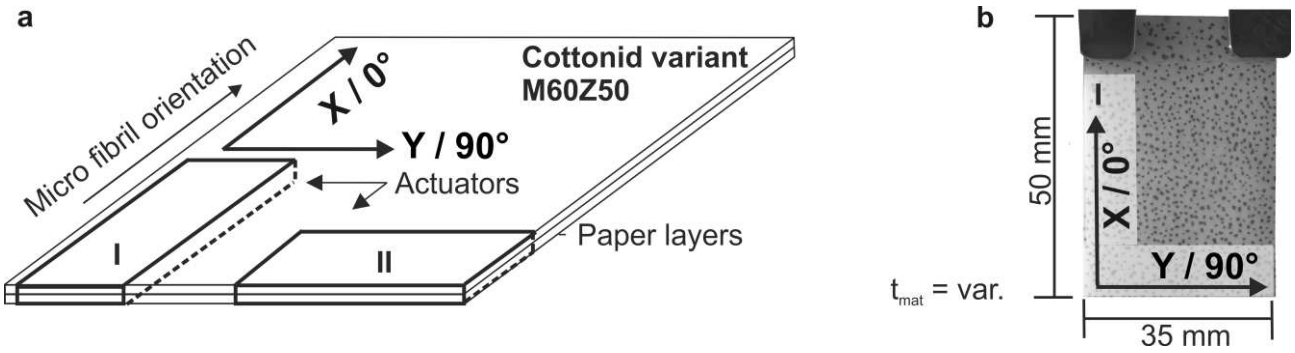

572

573 **Fig. 1**

574

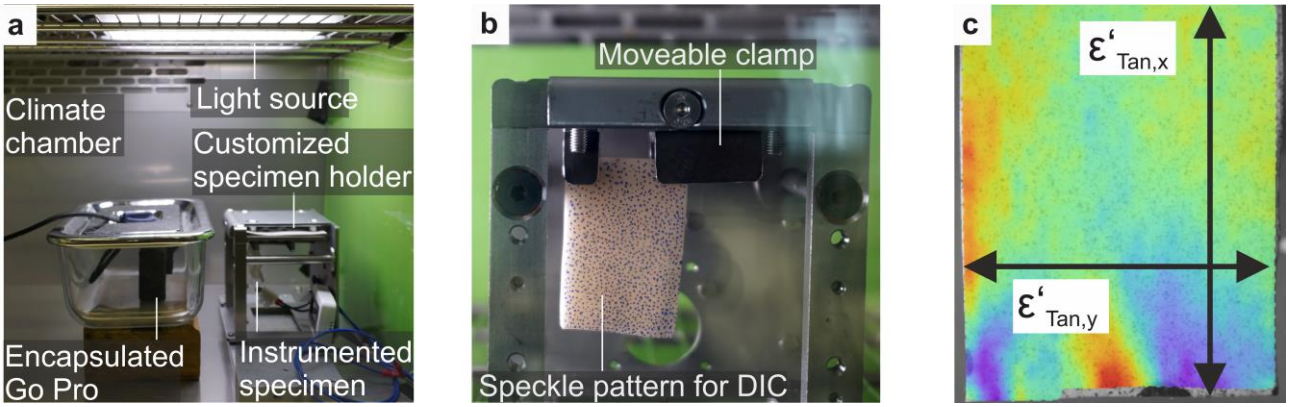

575

576 **Fig. 2**

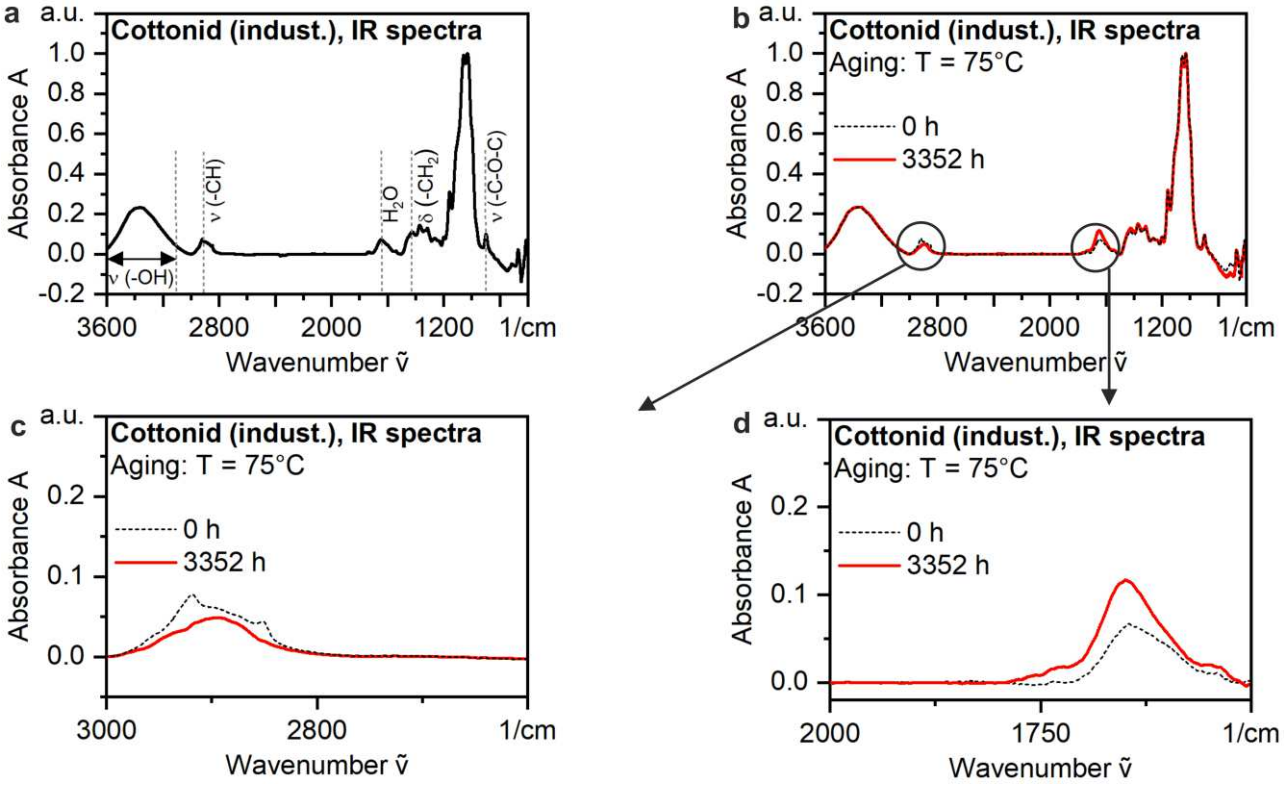
a
a.u.
Cottonid (indust.), IR spectra
Absorbance A
1.0
0.8
0.6
0.4
0.2
0.0
-0.2
ν (-OH)
ν (-CH)
H2O
δ (-CH2)
ν (-C-O-C)
3600
2800
2000
1200
1/cm
Wavenumber ṽ
b
a.u.
Cottonid (indust.), IR spectra
Aging: T = 75°C
0 h
3352 h
Absorbance A
1.0
0.8
0.6
0.4
0.2
0.0
-0.2
3600
2800
2000
1200
1/cm
Wavenumber ṽ
c
a.u.
Cottonid (indust.), IR spectra
Aging: T = 75°C
0 h
3352 h
Absorbance A
0.2
0.1
0.0
3000
2800
1/cm
Wavenumber ṽ
d
a.u.
Cottonid (indust.), IR spectra
Aging: T = 75°C
0 h
3352 h
Absorbance A
0.2
0.1
0.0
2000
1750
1/cm
Wavenumber ṽ

Fig. 3

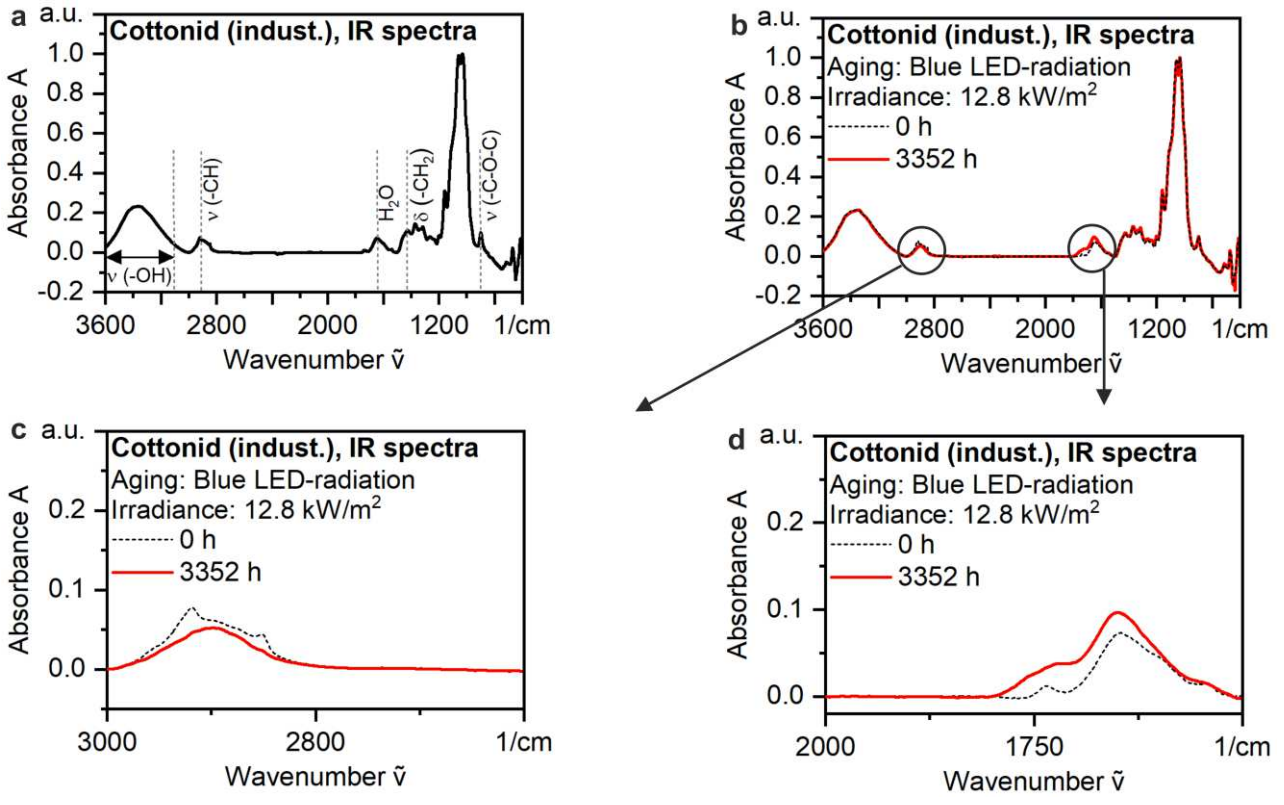
a
a.u.
Cottonid (indust.), IR spectra
Absorbance A
1.0
0.8
0.6
0.4
0.2
0.0
-0.2
ν (-OH)
ν (-CH)
H2O
δ (-CH2)
ν (-C-O-C)
3600
2800
2000
1200
1/cm
Wavenumber ṽ
b
a.u.
Cottonid (indust.), IR spectra
Aging: Blue LED-radiation
Irradiance: 12.8 kW/m2
0 h
3352 h
Absorbance A
1.0
0.8
0.6
0.4
0.2
0.0
-0.2
3600
2800
2000
1200
1/cm
Wavenumber ṽ
c
a.u.
Cottonid (indust.), IR spectra
Aging: Blue LED-radiation
Irradiance: 12.8 kW/m2
0 h
3352 h
Absorbance A
0.2
0.1
0.0
3000
2800
1/cm
Wavenumber ṽ
d
a.u.
Cottonid (indust.), IR spectra
Aging: Blue LED-radiation
Irradiance: 12.8 kW/m2
0 h
3352 h
Absorbance A
0.2
0.1
0.0
2000
1750
1/cm
Wavenumber ṽ

Fig. 4

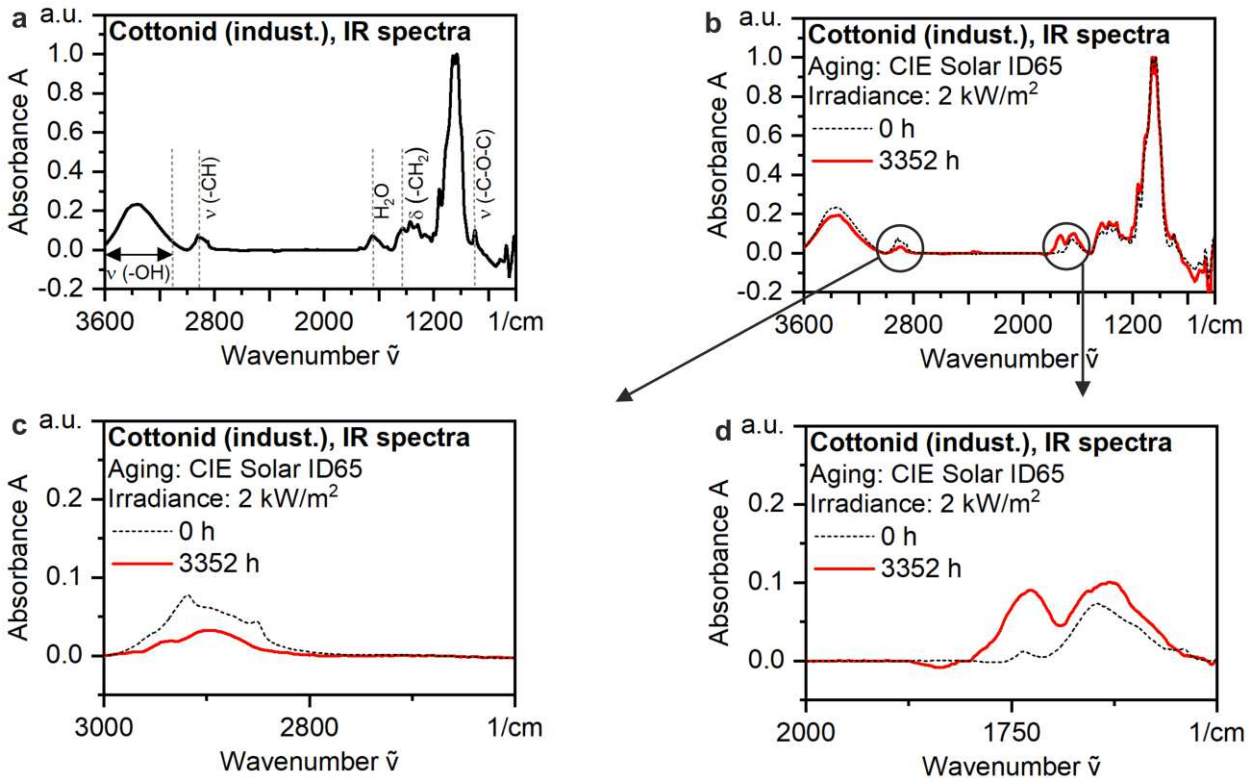

583

584 **Fig. 5**

585

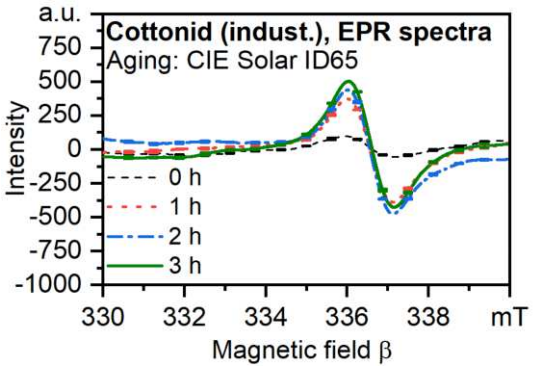

586

587 **Fig. 6**

588

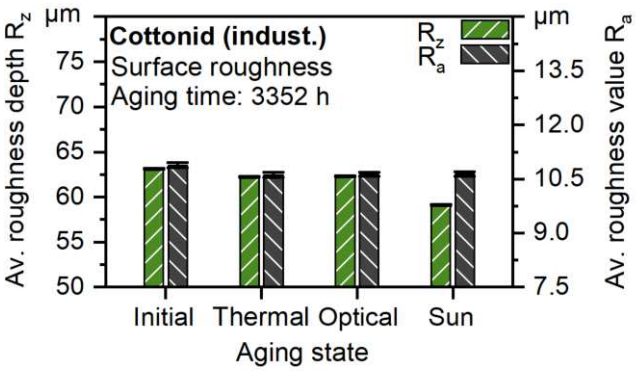

589

590 **Fig. 7**

591

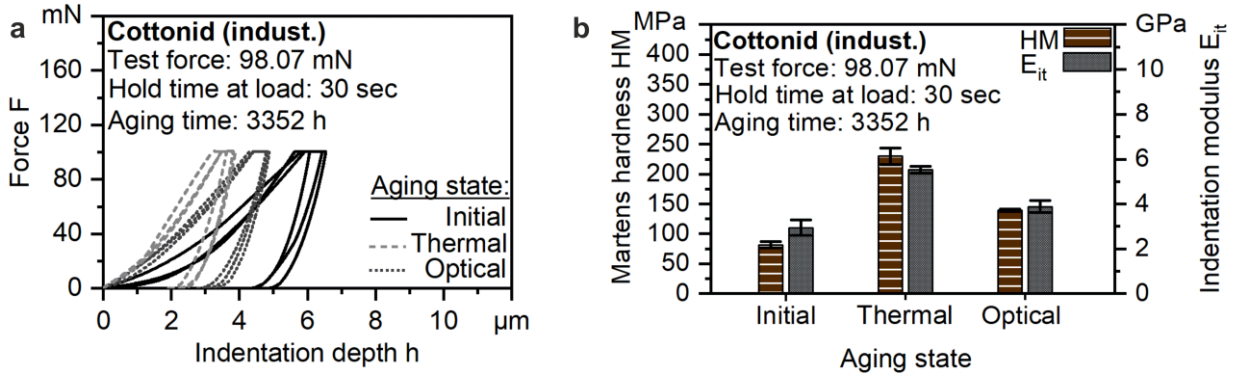

592

593 **Fig. 8**

594

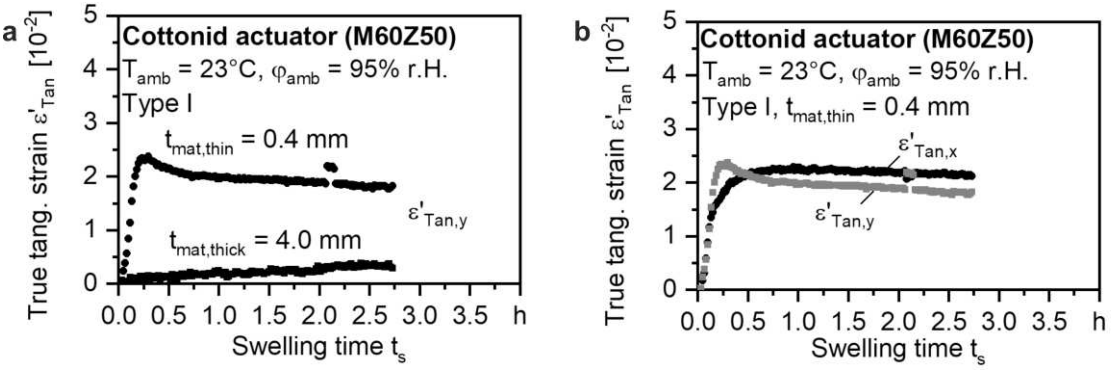

595

596 **Fig. 9**

597

598

599

600

601 **Tables**

602 **Tab. 1**

Cottonid variant	Cellulose source	Reaction time	Catalyst	Temperature
M60Z50	Cotton linters („M“)	60 sec	Zincdichloride solution („Z“)	50 °C

603

Figure and table captions

Fig. 1

Specimen preparation for actuation experiments: **a** Specimen location in Cottonid sheet according to manufacturing direction of paper layers, and **b** Cottonid actuator type I with speckled surface for strain measurements via digital image correlation (DIC) mounted in customized specimen holder

Fig. 2

a Test setup for actuation experiments in alternating climate chamber (MKF 115, Binder, Tuttlingen, Germany); **b** Cottonid specimen with speckled surface for strain measurements via digital image correlation (DIC) mounted in customized specimen holder; **c** Strain measurements on specimen's surface via DIC parallel ($\varepsilon'_{Tan,x}$) and perpendicular ($\varepsilon'_{Tan,y}$) to cellulose micro fibril orientation

Fig. 3

Infrared (IR) spectra of industrial Cottonid material (Ernst Krueger): **a** In initial condition with peak definition of raw material cellulose, and **b** Comparative evaluation of initial condition and after thermal aging at ~75°C for t_{aging} = 3352 h; Peak evolution due to thermal aging: **c** Close-up at $\tilde{\nu}$ = 2.900 cm^{-1}, and **d** Close-up at $\tilde{\nu}$ ~ 1.750 cm^{-1}

Fig. 4

Infrared (IR) spectra of industrial Cottonid material (Ernst Krueger): **a** In initial condition with peak definition of raw material cellulose, and **b** Comparative evaluation of initial condition and after optical aging (blue LED-radiation, irradiance: 12,8 kW/h) for t_{aging} = 3352 h; Peak evolution due to optical aging: **c** Close-up at $\tilde{\nu}$ = 2.900 cm^{-1}, and **d** Close-up at $\tilde{\nu}$ ~ 1.750 cm^{-1}

Fig. 5

Infrared (IR) spectra of industrial Cottonid material (Ernst Krueger): **a** In initial condition with peak definition of raw material cellulose, and **b** Comparative evaluation of initial condition and after optical aging (CIE solar ID65, irradiance: 2 kW/h) for t_{aging} = 3352 h; Peak evolution due to optical aging: **c** Close-up at $\tilde{\nu}$ = 2.900 cm^{-1}, and **d** Close-up at $\tilde{\nu}$ ~ 1.750 cm^{-1}

Fig. 6

Electron paramagnetic resonance (EPR) spectra of industrial Cottonid material (Ernst Krueger) in initial condition and after aging with standardized artificial solar irradiation (CIE solar ID65, irradiance: 2 kW/h) for increasing aging times

Fig. 7

Roughness measurements on surface of industrial Cottonid material (Ernst Krueger) in different aging stages

Fig. 8

Ultra-micro-hardness measurements on surface of industrial Cottonid material (Ernst Krueger) in different aging stages: **a** Force (F) - indentation depth (h) curves, and b Obtained values for Martens hardness HM and indentation modulus E_{it}

Fig. 9

Actuation tests on structurally optimized Cottonid variant M60Z50: **a** Influence of cellulose micro fibril orientation, and **b** Influence of material thickness t_{mat}

Tab. 1

Sample designation of structurally optimized Cottonid

Figures

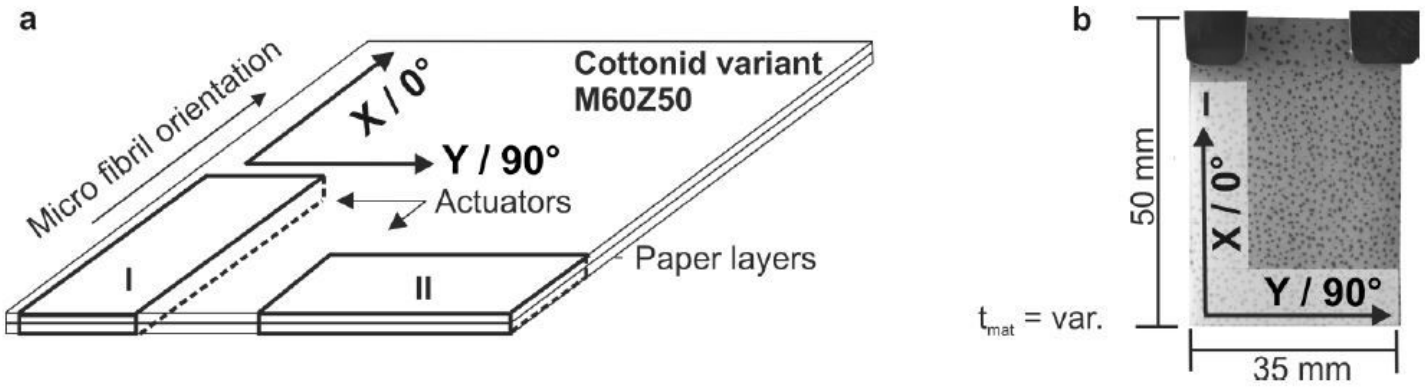

Figure 1

Specimen preparation for actuation experiments: a Specimen location in Cottonid sheet according to manufacturing direction of paper layers, and b Cottonid actuator type I with speckled surface for strain measurements via digital image correlation (DIC) mounted in customized specimen holder

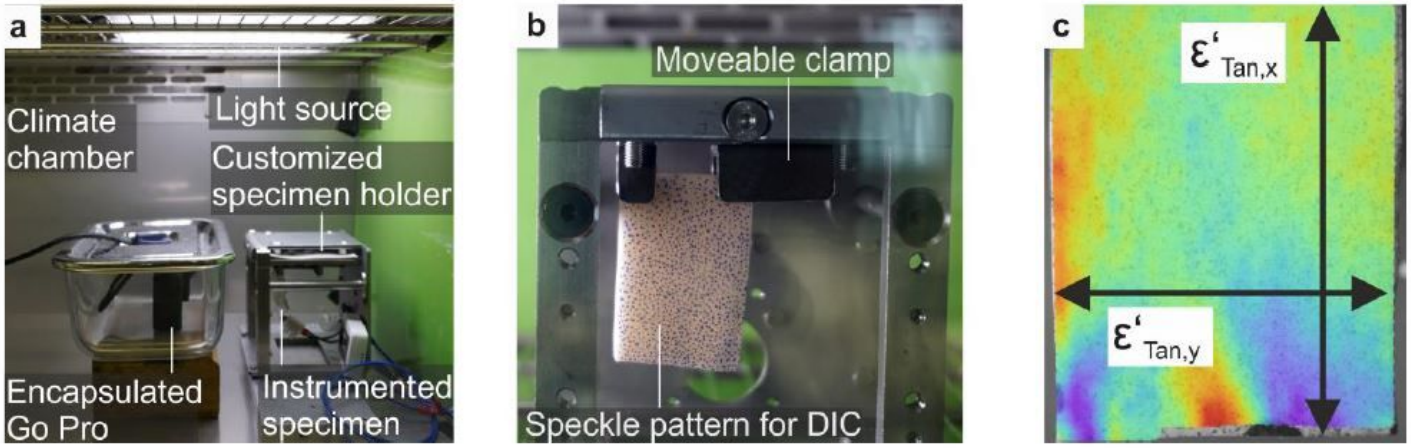

Figure 2

a Test setup for actuation experiments in alternating climate chamber (MKF 115, Binder, Tuttlingen, Germany); b Cottonid specimen with speckled surface for strain measurements via digital image correlation (DIC) mounted in customized specimen holder; c Strain measurements on specimen's surface via DIC parallel (ε'Tan,x) and perpendicular (ε'Tan,y) to cellulose micro fibril orientation

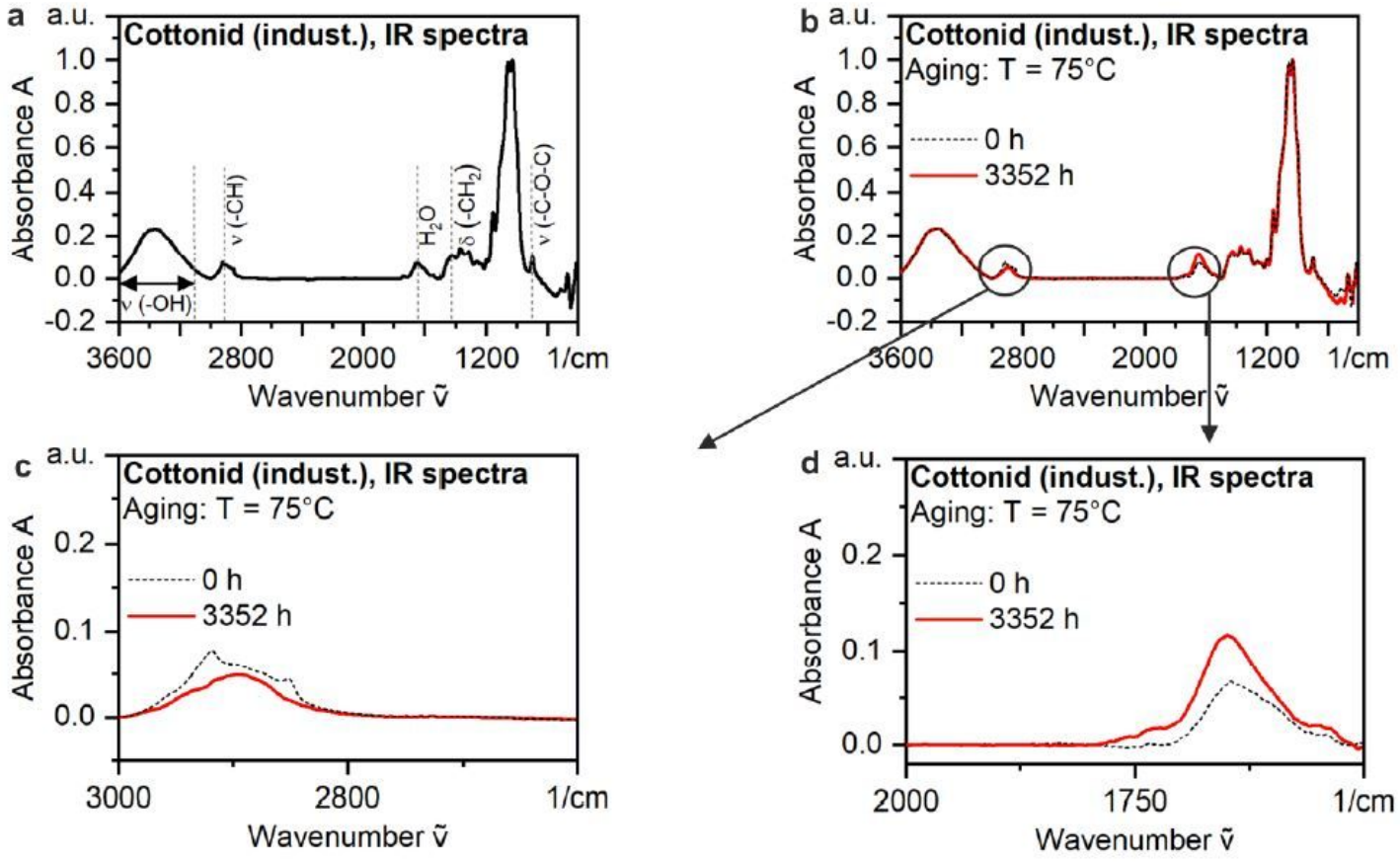

Figure 3

Infrared (IR) spectra of industrial Cottonid material (Ernst Krueger): a In initial condition with peak definition of raw material cellulose, and b Comparative evaluation of initial condition and after thermal aging at ~75°C for taging = 3352 h; Peak evolution due to thermal aging: c Close-up at ṽ = 2.900 cm-1, and d Close-up at ṽ ~ 1.750 cm-1

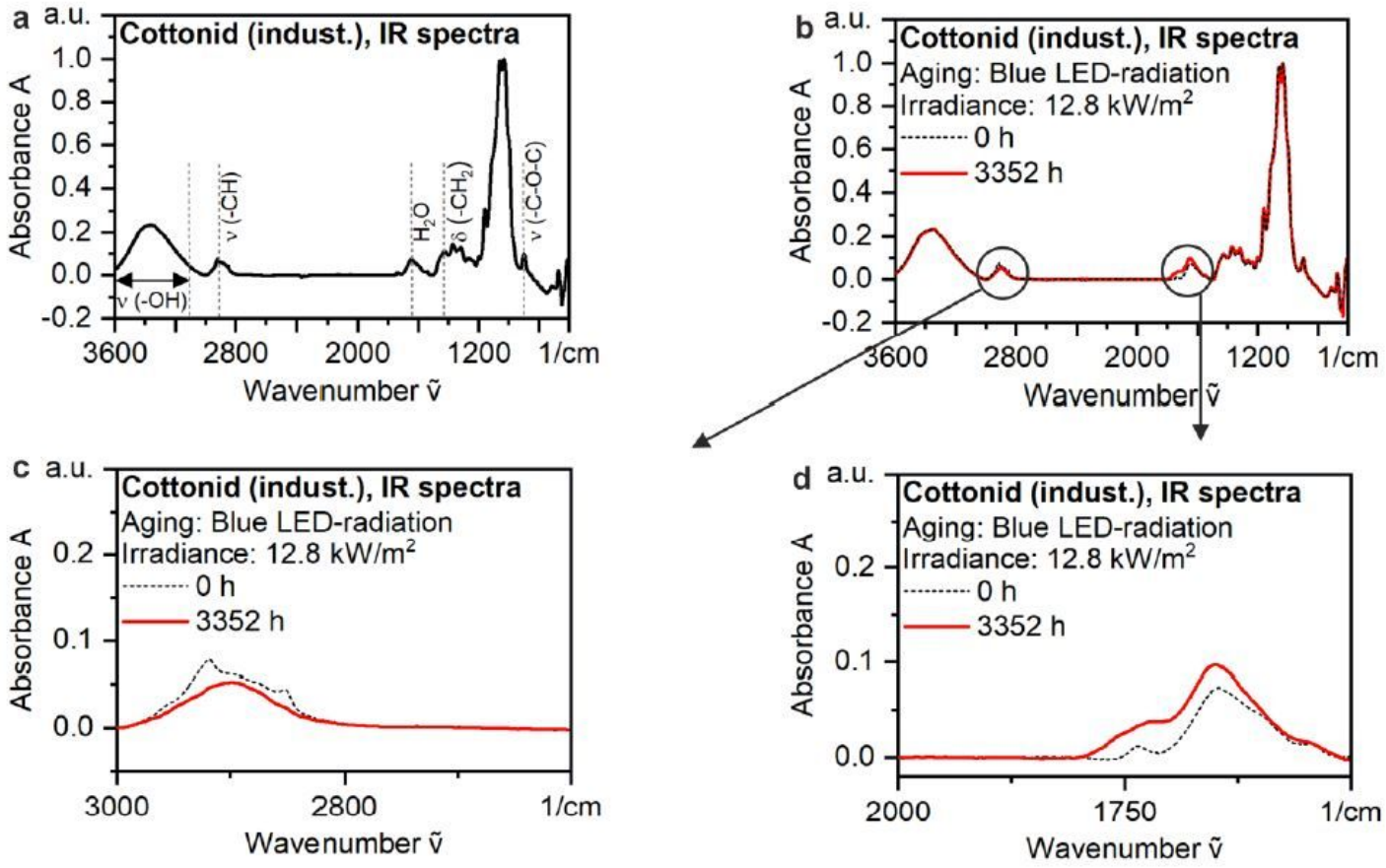

Figure 4

Infrared (IR) spectra of industrial Cottonid material (Ernst Krueger): a In initial condition with peak definition of raw material cellulose, and b Comparative evaluation of initial condition and after optical aging (blue LED-radiation, irradiance: 12,8 kW/h) for taging = 3352 h; Peak evolution due to optical aging: c Close-up at ṽ = 2.900 cm-1, and d Close-up at ṽ ~ 1.750 cm-1

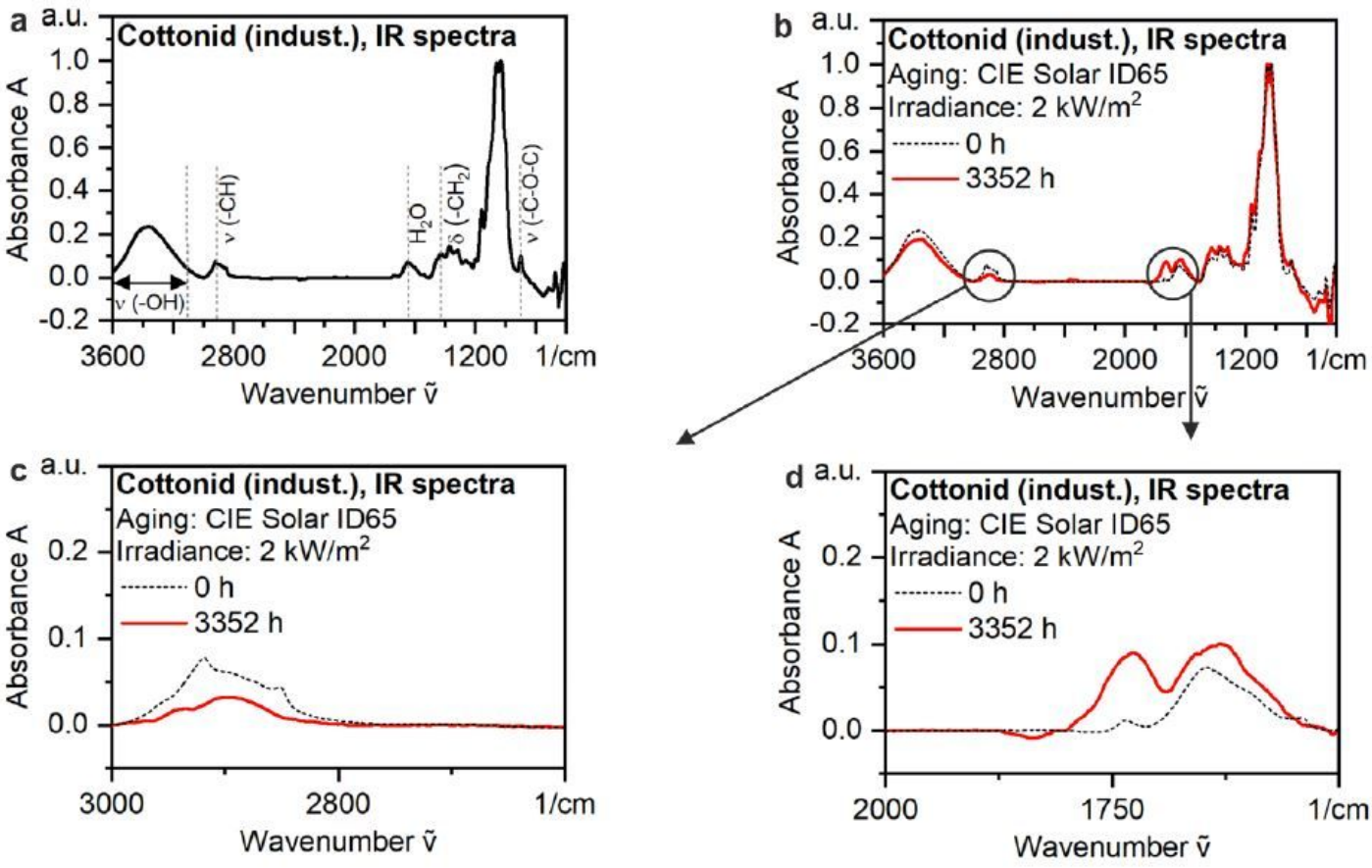

Figure 5

Infrared (IR) spectra of industrial Cottonid material (Ernst Krueger): a In initial condition with peak definition of raw material cellulose, and b Comparative evaluation of initial condition and after optical aging (CIE solar ID65, irradiance: 2 kW/h) for taging = 3352 h; Peak evolution due to optical aging: c Close-up at ṽ = 2.900 cm-1, and d Close-up at ṽ ~ 1.750 cm-1

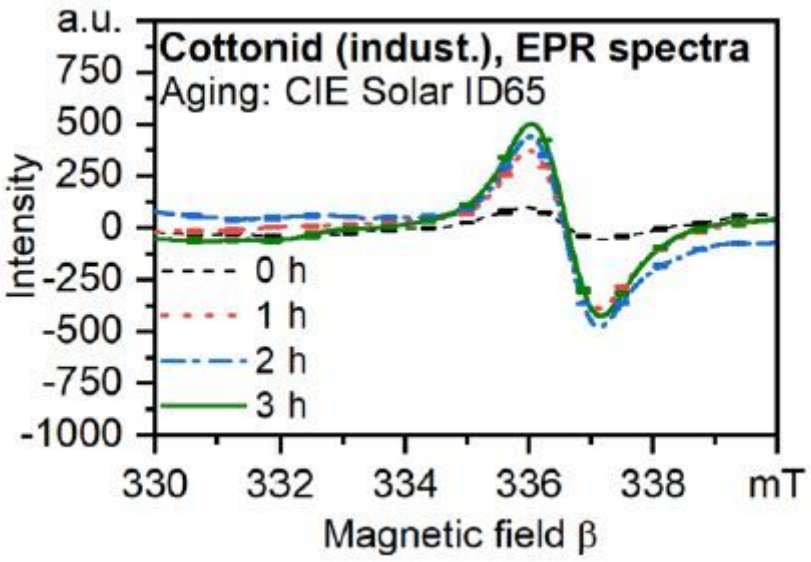

Figure 6

Electron paramagnetic resonance (EPR) spectra of industrial Cottonid material (Ernst Krueger) in initial condition and after aging with standardized artificial solar irradiation (CIE solar ID65, irradiance: 2 kW/h) for increasing aging times

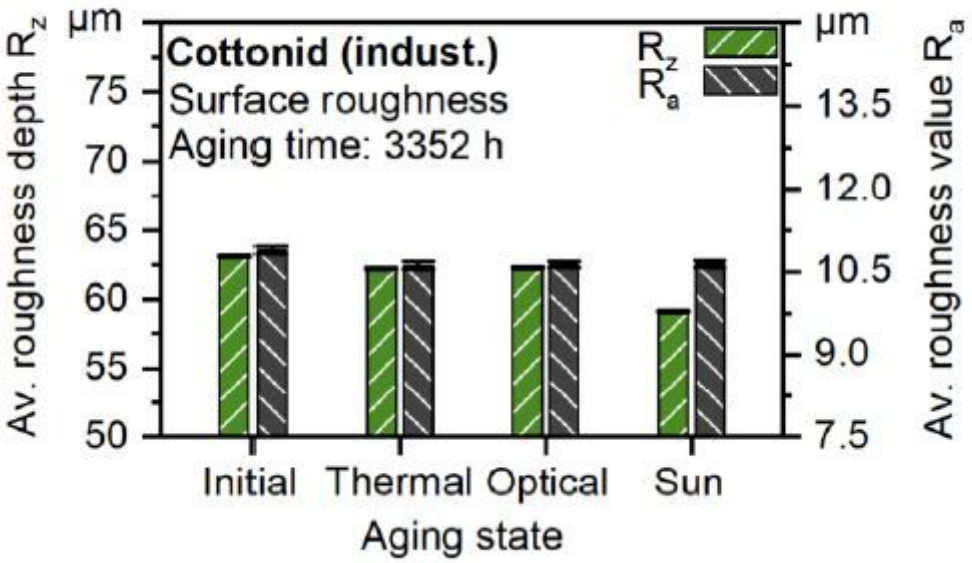

Figure 7

Roughness measurements on surface of industrial Cottonid material (Ernst Krueger) in different aging stages

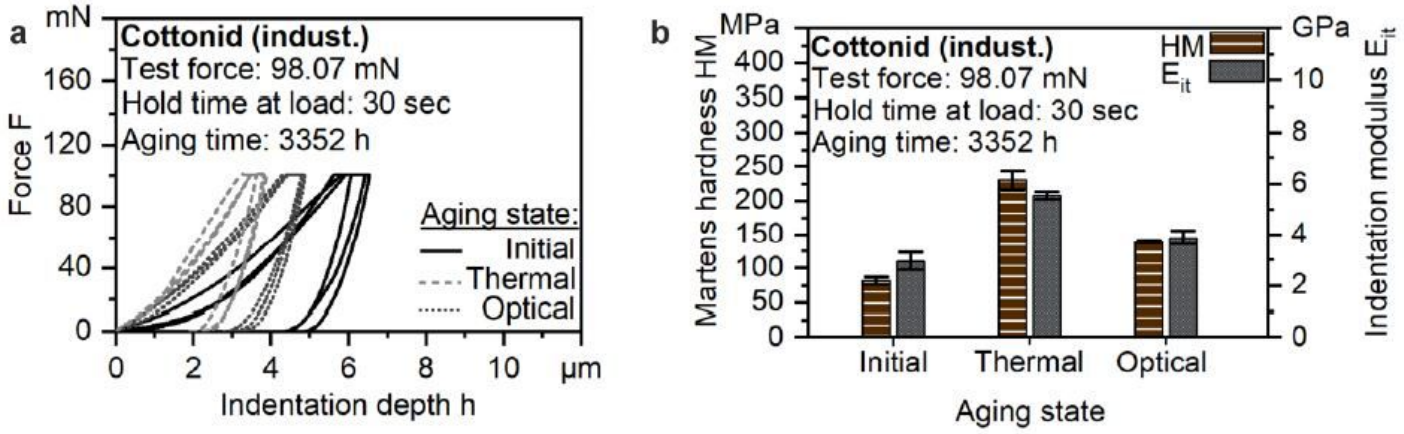

Figure 8

Ultra-micro-hardness measurements on surface of industrial Cottonid material (Ernst Krueger) in different aging stages: a Force (F) - indentation depth (h) curves, and b Obtained values for Martens hardness HM and indentation modulus Eit

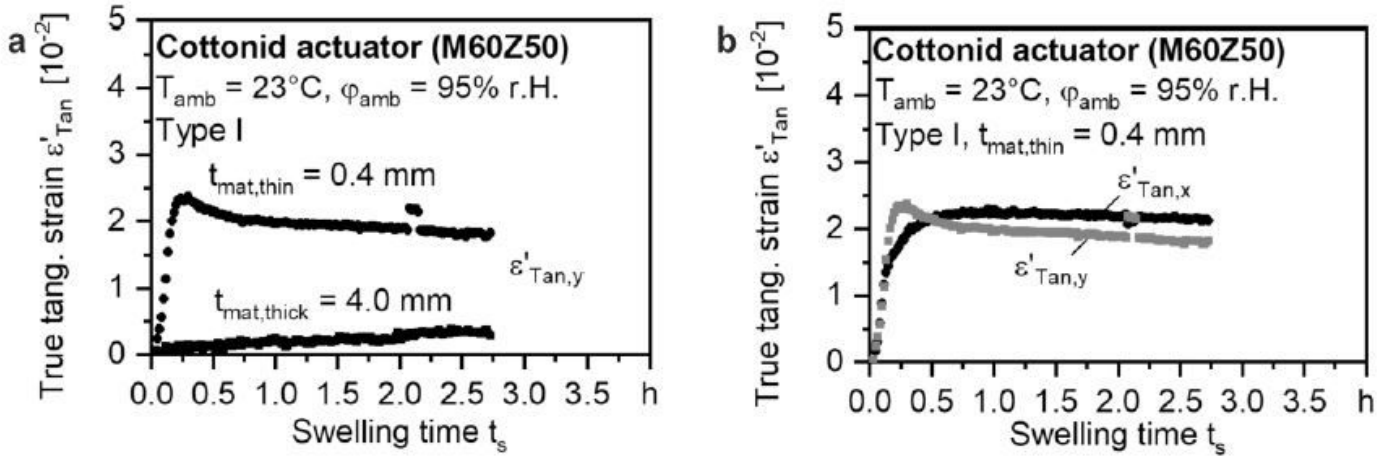

Figure 9

Actuation tests on structurally optimized Cottonid variant M60Z50: a Influence of cellulose micro fibril orientation, and b Influence of material thickness tmat